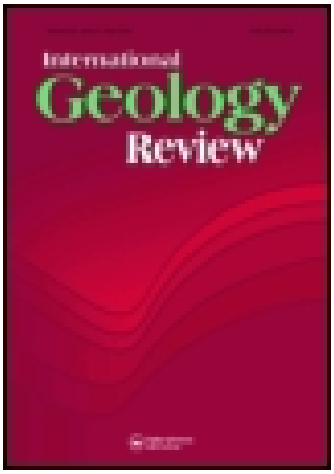

International Geology Review
Publication details, including instructions for authors and subscription information:
http://www.tandfonline.com/loi/tigr20

Differentiation of the Emeishan Flood Basalts at the Base and throughout the Crust of Southwest China

Dan Zhu [a] , Tai-Yi Luo [a] , Zhen-Min Gao [a] & Chen-Ming Zhu [a]
[a] Institute of Geochemistry, Chinese Academy of Sciences
Published online: 14 Jul 2010.

To cite this article: Dan Zhu , Tai-Yi Luo , Zhen-Min Gao & Chen-Ming Zhu (2003) Differentiation of the Emeishan Flood Basalts at the Base and throughout the Crust of Southwest China, International Geology Review, 45:5, 471-477, DOI: 10.2747/0020-6814.45.5.471

To link to this article: http://dx.doi.org/10.2747/0020-6814.45.5.471

International Geology Review, Vol. 45, 2003, p. 471–477.

Differentiation of the Emeishan Flood Basalts at the Base and throughout the Crust of Southwest China

DAN ZHU,[1] TAI-YI LUO, ZHEN-MIN GAO,

Open Laboratory of Ore Deposit Geochemistry, Institute of Geochemistry, Chinese Academy of Sciences, 73 Guanshui Road, Guiyang, Guizhou, 550002, People's Republic of China

AND CHEN-MING ZHU

Laboratory of High Temperature and High Pressure, Institute of Geochemistry, Chinese Academy of Sciences, 73 Guanshui Road, Guiyang, Guizhou, 550002, People's Republic of China

Abstract

The Emeishan flood basalt is a large igneous province (LIP) erupted in southwestern China during the Permian Triassic period. Seismic images of the deep crustal structure beneath the Emeishan large igneous province (ELIP) indicate unusually high seismic velocities (V_p = 7.1 – 7.8 km/s) at the base of the crust. The thickness of these high-velocity layers ranges from 8 km in the western section to 24 km in the east, and are generally interpreted as large igneous intrusions. In this paper, we use the petrological code MELTS to quantify the crystal fractionation of Emeishan primary melts at the base of the crust as they ascended to the surface. Using the thickness and the seismic velocity (V_p) of these high-velocity layers as constraints, MELTS rigorously calculates the amount and the composition of the fractionated solid phases and the major oxide concentrations in the residual liquids. The computed compositions of the residual liquids are rich in TiO_2 and FeO_{tot}, consistent with the observed compositions of most Emeishan basalts. Moreover, the calculated seismic velocities (V_p) of fractionated solid phases are also consistent with the geophysical observations. Mass balance calculation shows that the entire volume of the Emeishan basalts is about $8.9\times10^6 km^3$. The results also explain the absence of huge layered gabbro intrusions (V-Ti-magnetite deposits) in the west section of ELIP, and indicate that the east section is a potential mineral exploration region for V-Ti-magnetite deposits.

Introduction

FLOOD BASALTS are the largest volcanic events known on Earth. They are characterized by enormous volumes (~10^5–10^7 km^3) of relatively homogeneous tholeiitic basalts erupted in a relatively short time span (1–2 m.y.) (Coffin and Eldholm, 1994; Hooper, 2000). Several researchers have established that the Emeishan flood basalts (EFB) in particular are consistent with emplacement by a mantle plume (Chung and Jahn, 1995; Chung et al., 1998; Xu and Chung, 2001; Xu et al., 2001a). The Emeishan large igneous province (ELIP), which consists of massive flood basalts and numerous contemporaneous mafic intrusions, culminated in a main stage of flood magmatism at ~251–253Ma (Lo et al., 2002). The primary melts of the Emeishan flood basalts (EFBs) are thought to be picritic (Chung and Jahn,1995; Xu and Chung, 2001; Xu et al., 2001a). However, most basaltic lavas from the Emeishan LIP (ELIP) are more evolved, with MgO ≈7% (Zhang et al., 1988; Xu et al., 2001a). They are far from the expected composition of melts in equilibrium with mantle peridotites (Cox, 1980). The discrepancy between the composition of the primary picritic melts and the observed compositions of the erupted lavas indicates that primary mantle melts underwent significant crystal fractionation before being erupted. According to Cox (1980), primary picritic magmas may have ponded and fractionated near the Moho due to the density contrast between picritic magma and crust. This process produces ultramafic cumulates and residual low-MgO basaltic magma. The fractionated cumulates and intrusions would be expected to cause underplating and thickening of the crust — features that should be detectable by geophysical observations. The high-seismic-velocity layers (V_p = 7.1 – 7.8 km/s) at the base of the crust beneath this province (Liu et al., 2000; Yuan, 1989) may correspond to the underplated cumulate pile

[1]Corresponding author; email: zhudan-gy@163.net

from magmas derived from Emeishan mantle plumes. Geochemical evidence also suggests that the high-seismic-velocity layers underlying the ELIP were formed by EFB magmas. Cenozoic mafic potassic and ultrapotassic magmas in the ELIP (Xu et al., 2001b; Chung et al., 1997; Deng et al., 1998) are considered to be derived from the high-seismic-velocity-layers, which are called the "crust-mantle mixed layers" (Deng et al., 1998), and the Pb isotope age inherited by these magmas is 220~250 Ma (Deng et al., 1998), consistent with the age of the EFB magmas (Lo et al., 2002).

There is now a growing body of seismic data on the deep crustal structure of hotspot tracks, such as Hawaii and the Marquesas Islands; of oceanic plateaus such as Ontong Java; and of continental flood basalt provinces, such as the Columbia River Plateau (Farnetani et al., 1996 and references therein). The seismic data consistently indicate crustal thickening and the existence of high-velocity layers at the base of the crust. Farnetani et al. (1996) have established a model for these high-velocity layers. However, their results are not accurate, because the primary melts used are taken from melting experiments that are not appropriate for the specific geological process of lower-crustal flood basalt fractionation.

In this paper we use the Emeishan primary melt recently found (Xu and Chung, 2001; Xu et al., 2001a), and the petrological code MELTS (Ghiorso and Sack, 1995) to quantify the crystal fractionation of Emeishan primary melts at the base of the crust (at the Moho) before they ascended to the surface. The results of the crystal fractionation calculation are consistent with petrological characteristics of the EFB magmas, show the compositions of the high-seismic-velocity layer beneath the ELIP, and also predict the tectonic position of V-Ti-magnetite deposits. The calculation also provides a mass balance that allows an estimate of the entire volume of EFB material, erupted or intruded.

Background

The ELIP is located along the western margin of the Yangtze craton in southwestern China. The basement of the ELIP consists mainly of metamorphic rocks of Middle Proterozoic age. The Emeishan basalts are exposed in a rhombic area of ~250,000 km^2 within Yunnan, Sichuan, and Guizhou provinces (detailed descriptions are available in Zhang et al., 1988). The ELIP has been divided into three subsections termed the west, middle, and east sections (Zhang et al., 1988). The Red River shear zone is considered as its western boundary (Zhang et al., 1988). The Qinghe and Chenghai faults mark boundaries of the west section and middle sections of the ELIP, whereas the Ganluo-Xiaojiang faults divide the middle from the east section (Fig. 1). Thickness of EFB varies from over 5000 m in the west (i.e., the Binchuan Profile in Yunnan Province) to several hundred meters in the east. However, the thickest section may originally have been in the middle section, now removed due to intense erosion during the Late Permian–Early Triassic. From the results of paleocontinental reconstruction, the middle section of the ELIP overlay the high-standing core of the Kangdian paleocontinent during Late Permian–Early Triassic time, and the estimated thickness of its erosion is over 5 km; in contrast, the west and east sections are delta to littoral facies (Pan et al., 1987). So the initial thickness of the basalt sections is estimated at 5 km and 8 km, respectively, in the west and middle sections of this province.

The high-seismic-velocity layers beneath the ELIP have two sublayers with velocities of 7.1–7.5 km/s and 7.5–7.8 km/s, respectively. These two layers together (V_p = 7.1 – 7.8 km/s) reach a thickness of 25 km beneath the middle section of this province, thinning to 8 km beneath the west section. The east section has a stable thickness of 20 km (Liu et al. 2000).

The EFB is classified into two major magma types: high-Ti (HT) and low-Ti (LT) basalts. The HT basalts form the main body of EFBs, and are characterized by high TiO_2 (3.65–5%), high Fe_2O_3 (12.7–16.4%), and low MgO (<7%) contents (Xu et al., 2001a).

Methods

We use the thermodynamic code MELTS (Ghiorso and Sack, 1995) to model fractional crystallization of the EFBs. The initial composition of the primary melts of EFBs is in Table 1 (Chung and Jahn, 1995; Xu et al., 2001a). The depth of the Moho beneath the ELIP is presently about 40 km(≈12 kbar), but this is the result of subsequent folding (Cong, 1988). Instead we estimate the pressure of crystallization using Putirka's thermobarometer (Putirka et al., 1996; Putirka, 1997) and data from Zhang (Zhang et al., 1988). The results show two major average pressure values: (1) 6 kbar (≈20

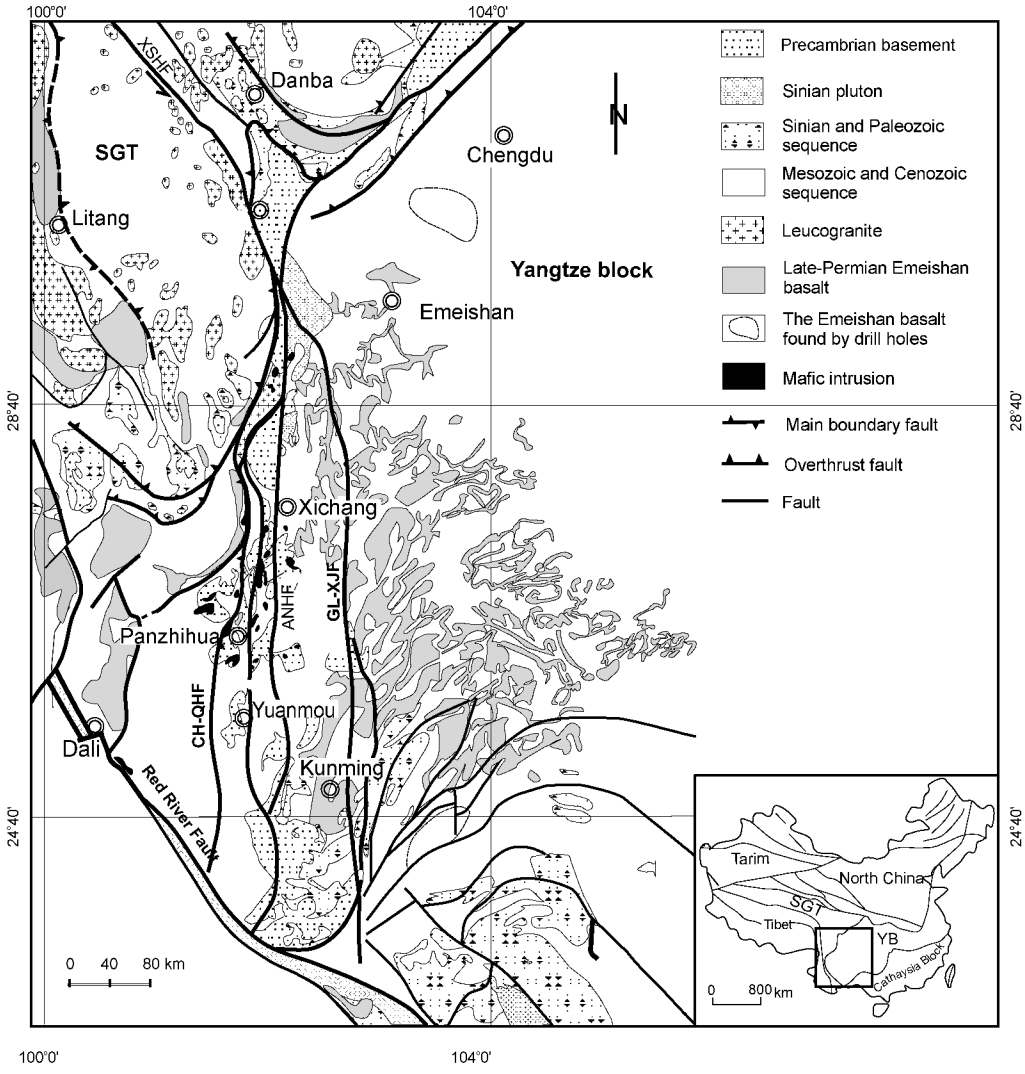

FIG. 1. Geological map of Southwestern China, showing the distribution of the EFBs and contemporaneous mafic intrusions within the ELIP (South China) (Modified from Zhou et al., 2002 and Song et al., 2001). The lower right inset illustrates distribution of major terranes in China and study area (modified after Chung and Jahn, 1995). Abbreviations: CH-QHF = Chenghai-Qinghe fault; XSHF = Xianshuihe fault; ANHF=Anninghe fault; GL-XJF = Ganluo-Xiaojiang fault; SGT = Songpan-Ganze Teerane; YB = Yangze Block.

km, presumably representing the depth of Moho at that time); and (2) 1 kbar (representing a subordinate high-level crystallization of EFBs in the upper crust). The oxygen fugacity used in the calculation is the quartz-fayalite-magnetite (QFM) buffer. This condition was selected because most tholeiitic basalts are considered to have crystallized under these f_{O2} conditions (Walker et al., 1979; Helz and Thornber, 1987).

Results and Discussion

The results of fractional crystallization using MELTS are shown in Table 1 and Figure 2. The

TABLE 1. Calculation Results

Oxide	SiO_2	TiO_2	Al_2O_3	FeO[1]	MgO	CaO	Na_2O	K_2O	P_2O_5	Fraction of each phase					Density
										Ol	Opx	Cpx	Sp	melt	g/cm^3
Primary melt[2]	46.75	2.88	8.12	12.73	17.20	9.22	1.43	0.93	0.24						3.19
Intermediate liquid[3]	44.10	4.55	11.92	15.29	8.55	10.68	2.29	1.53	0.40						3.15
Final liquid[4]	42.60	5.63	14.16	17.17	5.7	8.25	3.00	2.12	0.55						3.11
(Vp = 7.5–7.8 km/s) layer	48.91	0.45	4.41	9.90	29.66	5.90	0.31	0.11	0.03	22.1	41.7	28.1	1.0	7.0[5]	3.19
(Vp = 7.1 – 7.5 km/s) layer	46.44	1.49	9.28	11.22	15.44	14.36	0.89	0.32	0.08			82.9	2.1	15.0[6]	3.19

[1]Total iron.
[2]Primary melt is from Xu and Chung (2001).
[3]The evolved liquid after the primary melt has undergone 40% crystal fractionation.
[4]The evolved liquid after the primary melt has undergone 54% crystal fractionation.
[5]The fraction of the trapped intermediate composition liquid.
[6]The fraction of the trapped final composition liquid.

calculated trends of Al_2O_3, $Na_2O + K_2O$ and CaO vs. MgO are perfectly consistent with the evolved trend analyzed for the EFBs (Figs. 2B–2D). CaO increases with decreasing MgO as a result of olivine and orthopyroxene fractional crystallization, and then decreases as clinopyroxene reaches the liquidus at about MgO = 10.3%. The discrepancy between the calculated and observed trends in SiO_2 (Fig. 2A) is due to known systematic errors in MELTS. That the calculated trends of Fe_2O_3 (total) and TiO_2 lie above the observed trends suggests that the composition in the selected primary melt was atypically high in these oxides, because the calculated trends are parallel to the data arrays (Figs. 2E and 2F). Moreover, the observed microphenocrysts of magnetite and Ti-magnetite in most of the EFBs indicate that low-pressure crystal fractionation reduces both TiO_2 and FeO* in the EFBs.

Plagioclase does not appear as a liquidus phase during fractional crystallization at 6 kbar. This is consistent with the absent or slightly negative Eu anomalies (Cong, 1988) in the EFBs and the monotonic increase in Al_2O_3 with decreasing MgO during crystal fractionation (Fig. 2B). The observed phenocrysts of plagioclase in most of the EFBs are due to minor low-pressure crystallization of plagioclase (plagioclase is the main liquidus phase of the residual melt when brought to low pressure). However, phenocrysts of plagioclase were not separated from the residual liquid due to the high density of the residual liquid (the density of the ferrobasaltic residual liquid at 1209°C and 6 kbar is 2.91 g/cm^3, whereas the density of plagioclase is 2.64 g/cm^3).

The fractionated phases in the model of the EFB calculation yield a cumulate with calculated seismic velocities of 7.60–7.85 km/s (according to the averaging method of Farnetani et al., 1996). These values are at the high end of the observed seismic velocities of 7.1–7.8 km/s (assuming that the effects of pressure and temperature on seismic velocity counteract with each other) (Rudnick and Fountain, 1995). However, petrography of layered mafic intrusions shows that mafic cumulus can trap 5–30 volume percent liquid (Kerr and Tait, 1986; Miller and Ripley, 1996). If the two high seismic velocity layers of 7.1–7.5km/s and 7.5–7.8 km/s trapped 15% and 7% liquid, respectively, the calculated values would be approximately equal to the measured velocities. The compositions of estimated high-seismic-velocity layers obtained by mixing the model cumulate composition with residual liquid to obtain the appropriate seismic velocities are shown in Table 1. The two layers are pyroxenite (V_p = 7.1 – 7.5 km/s) and olivine-pyroxenite (V_p = 7.5 – 7.8 km/s), respectively.

The results of the mass balance calculation show the volume proportion of the solid phases and residual liquid for the west and middle sections of the ELIP (Fig. 3). Volume proportions are approxi-

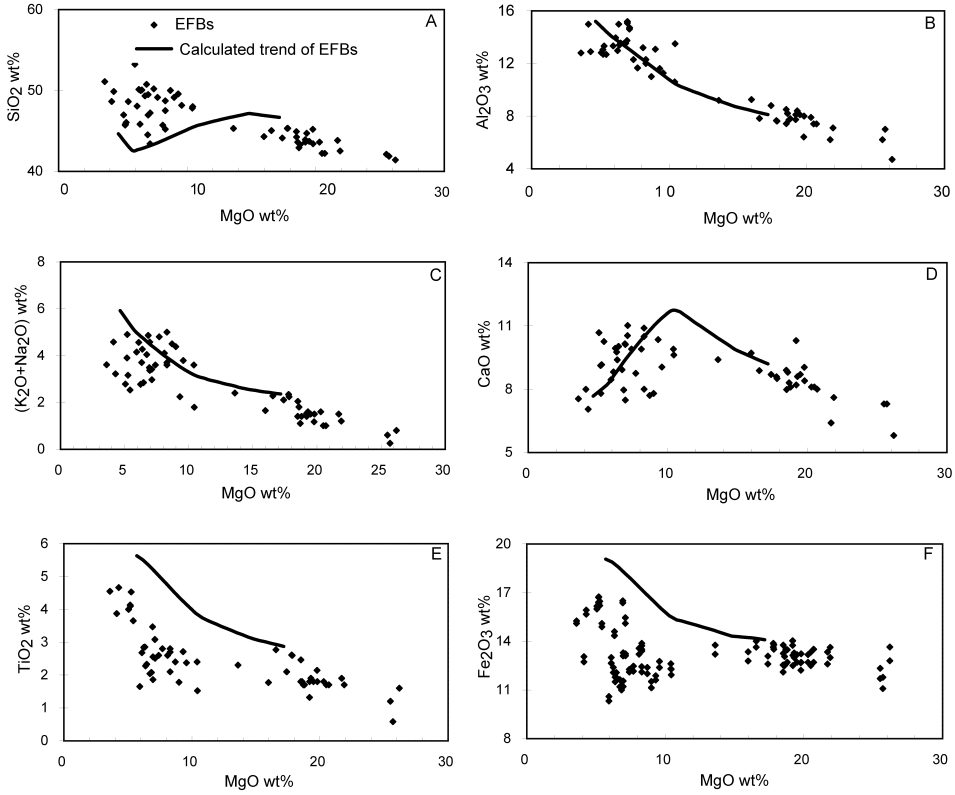

FIG. 2. Variation diagrams for major oxides plotted against MgO for the EFB magmas and the evolved trend of calculation at 6 kbar and the QFM buffer. All data of the EFB magmas are from Chung and Jahn (1995); Xu et al., 2001c; and Song et al., 2001).

mately equal to the mass proportions due to the similar densities of each phase (see Table 1). The primary magmas have undergone 54% fractional crystallization at the Moho and the fractionated phases formed the high seismic velocity layers with a thickness of 8 km and 24 km in the west and the middle sections, respectively. After subtracting the trapped liquid, the total residual mass is about 44% of the total mass, which is the sum of the basalts and the intrusions in the upper crust. The initial thickness of basalt in the profile in the west and middle sections is thought to be 5 km and 8 km (see above), which are 35% and 19% of total mass, respectively. Assuming basalts and intrusions have similar densities, the mass fraction of intrusions in the upper crust is 9% and 25% and the "thickness" of the intrusions in the upper crust will be 1 km and 12 km in the west and middle sections, respectively (Fig. 3). These calculated results are consistent with observed facts: several huge layered gabbro intrusions (V-Ti-magnetite deposits, such as Panzhihua, Baima, Taihe and Hongge) are present in the middle section, whereas only small intrusions occur in the west (Yao et al., 1993). The east section has a thickness of 20 km of high-seismic-velocity layers, and is a potential mineral exploration target for V-Ti-magnetite deposits).

The average thickness of high-seismic-velocity layers is 20 km, and the total area of ELIP is ~250.000 km^2. So using the above calculating methods, the entire volume of Emeishan basalts is about 8.9×10^6 km^3, and the volume of the eruptive basalts and associated intrusions in the upper crust is 3.9×10^6 km^3. This value is apparently much greater than the 0.3×10^6 km^3 estimated by Xu et al. (2001a) based on preserved outcrop, only because

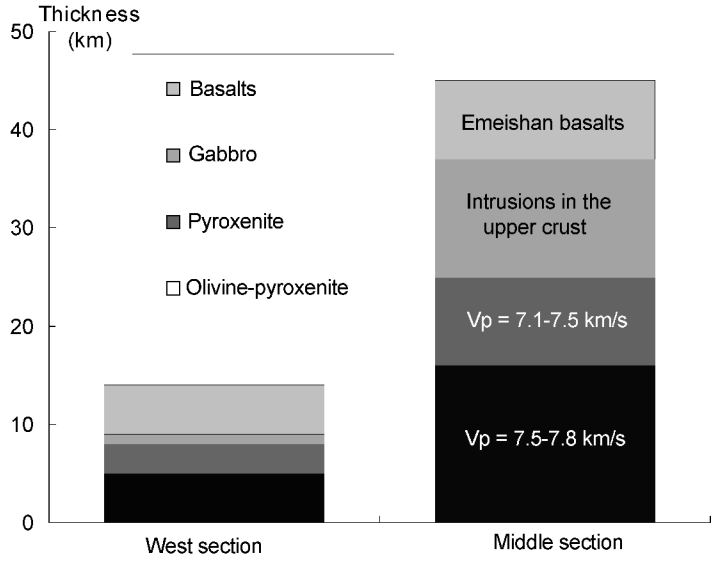

FIG. 3. Volume proportion of the solid phase and the residual liquid for the west and middle sections of the ELIP (shown as thickness). Volume proportion is approximately equal to the mass proportion due to the similar density of each phase.

our estimate accounts for erosion as well as associated intrusions.

Conclusions

The crystal fractionation calculations of the EFBs using MELTS show that the primary magma underwent about 54% differentiation at the base of crust and that the fractionated solid phases are consistent with the high-seismic-velocity layers in the lower crust if some trapped melt was retained in the cumulates. The compositions of the residual liquid are rich in TiO_2 and FeO_{tot}, consistent with most of the analyzed compositions of Emeishan basalts after a small amount of subsequent low-pressure plagioclase and oxide fractionation. Mass balance calculations show that the entire volume of Emeishan basalts is about 8.9×10^6 km^3. Moreover, the results explain the occurrence of huge layered gabbro intrusions (V-Ti-magnetite deposits) in the middle section and their absence in the west section of ELIP, and predict that the east section is a potential target for V-Ti-magnetite exploration.

Acknowledgments

We are grateful to Dr. Paul Asimov for comments that helped to improve an earlier draft of the manuscript. We thank Zhou Mei Fu, Xu Yi Gang, Chung Sun Lin, and Song Xie Yan for information regarding relevant literature. Paul Asimow and Mark Ghiorso are thanked particularly for their patient guidance in using the MELTS program. We are grateful to Keith Putirka for his careful help with the use of his thermobarometry calculations. The study benefited from financial support by the Chinese Academy of Sciences (KZCX2-101 and KZCX3-SW-125) and the Natural Science Foundation of China (grant 40274027).

REFERENCES

Chung, S. L., Lee, T. Y., Lo, C. H., Wang, P. L., Chen, C. Y., Yem, N. T., Hoa, T. T., and Wu, G. Y, 1997, Intraplate extension prior to continental extrusion along the Ailao Shan–Red River shear zone: Geology, v. 25, p. 311–314.

Chung, S. L., and Jahn, B. M., 1995, Plume lithosphere interaction in generation of the Emeishan flood basalts at the Permian Triassic boundary: Geology, v. 23, p. 889–892.

Chung, S. L., Jahn, B. M., Wu, G. Y., Lo, C. H., and Cong, B. L., 1998, The Emeishan flood basalt in SW China: A mantle plume initiation model and its connection with continental break-up and mass extinction at the Permian–Triassic boundary, *in* Flower, M. F. J., et al.,

eds., Mantle dynamics and plate interaction in East Asia: American Geophysical Union, Geodynamic Series, v. 27, p. 47–58.

Coffin, M. F., and Eldholm, O., 1994, Large igneous provinces: Crustal structure, dimensions, and external consequences: Reviews of Geophysics, v. 32, p. 1–36.

Cong, B. L., 1988, Formation and evolution of Eastern Part rift: Beijing, China, Science Publishing House, p. 158–195.

Cox, K. G., 1980, A model for flood basalt volcanism: Journal of Petrology, v. 21, p. 629–650.

Deng, W. M., Huang, X., and Zhong, D. L., 1998, Alkali-rich porphyry and its relation with intraplate deformation of North part of Jinsha River belt in Western Yunnan, China: Science in China, v. 41, p. 111–117.

Farnetani, C. G., Richards, M. A., and Ghiorso, M. S., 1996, Petrological models of magma evolution and deep crustal structure beneath hotspots and flood basalt provinces: Earth and Planetary Science Letters, v. 143, p. 81–94.

Ghiorso, M. S., and Sack, R. O., 1995, Chemical mass transfer in magmatic processes IV. A revised and internally consistent thermodynamic model for the interpolation and extrapolation of liquid-solid equilibria in magmatic systems at elevated temperatures and pressures: Contributions to Mineralogy and Petrology, v. 119, p. 197–212.

Helz, R. T., and Thornber, C. R., 1987, Geothermometry of Kilauea Iki lava lake, Hawaii: Bulletin of Volcanology, v. 49, p. 651–668.

Hooper, P. R., 2000, Flood basalt provinces, *in* Sigurdsson, H., et al., eds., Encyclopedia of volcanoes: San Diego, CA, Academic Press, p. 345–359.

Kerr, R. C., and Tait, S. R., 1986, Crystallization and compositional convection in a porous medium with application to layered igneous intrusions: Journal of Geophysical Research, v. 91, p. 3591–3608.

Liu, J. H., Liu, F. T., He, J. S., Cheng, H., and You, Q. Y, 2000, The tomographic research of Pan Xi ancient rifting—conclusion inferred from the structure and the evolution of the crust-mantle: Science in China (Series D, supplement), v. 30, p. 9–15 (in Chinese).

Lo, C. H., Chung, S. L., Lee, T. Y., and Wu, G. Y., 2002, Age of the Emeishan flood magmatism and relations to Permian–Triassic boundary events: Earth and Planetary Science Letters, v. 198, p. 449–454.

Miller, J. D., Jr., and Ripley, E. M., 1996, Layered intrusions of the Duluth complex, *in* Cawthorn, R. G., ed., Layered intrusions: Amsterdam, Netherlands, Elsevier, p. 257–301.

Pan, X. N, Zhao, J. X., and Zhang, X. Y., 1987, Tectonics and rifting in the Kangdian Region, Kangdian ancient continental rifting belt: Chong Qing, China: Chong Qing Press, p. 169–214 (in Chinese with English abstract).

Putirka, K., 1997, Magma transport at Hawaii: Inferences based on igneous thermobarometry: Geology, v. 25, p. 69–72.

Putirka, K., Johnson, M., Kinzler, R., Longhi, J. and Walker, D., 1996, Thermobarometry of mafic igneous rocks based on clinopyroxene-liquid equilibria, 0–30 kb: Contributions to Mineralogy and Petrology, v. 123, p. 92–108.

Rudnick, R. L., and Fountain, D. M., 1995, Nature and composition of the continental crust: A lower crustal perspective: Reviews of Geophysics, v. 33, p. 267–309.

Song, X. Y., Zhou, M. F., Hou, Z. Q., Cao, Z. M., Wang, Y. L., and Li, Y. G., 2001, Geochemical constraints on the mantle source of the upper Permian Emeishan continental flood basalts, southwestern China: International Geology Review, v. 43, p. 213–225.

Walker, D., Shibata, T., and DeLong, E., 1979, Abyssal tholeiites from the Oceanographer Fracture Zone II. Phase equilibria and mixing: Contributions to Mineralogy and Petrology, v. 70, p. 111–125.

Xu, Y. G., and Chung, S. L., 2001, The Emeishan Large Igneous Province: Evidence for mantle plume activity and melting conditions: Geochimica, v. 30, p. 1–9 (in Chinese with English abstract).

Xu, Y. G., Chung, S. L., Jahn, B. M., and Wu, G. Y., 2001a, Petrologic and geochemical constraints on the petrogenesis of Permian–Triassic Emeishan flood basalts in southwestern China: Lithos, v. 58, p. 145–168.

Xu, Y. G., Menzies, M. A., Thirlwall, M. F., and Xie, G. H., 2001b, Exotic lithosphere mantle beneath the western Yangtze craton: Petrogenetic links to Tibet using highly magnesian ultrapotassic rocks: Geology, v. 29, p. 863–866.

Yao, P. H., Wang, K. N., Du, C. L., Lin, Z. H., and Song, X., 1993, Records of China's iron ore deposits: Beijing, China, Metallurgical Industry Press (in Chinese).

Yuan, X. C., 1989, On the deep structure of the Kang-dian rift: Acta Geologica Sinica, v. 63, p. 1–13 (in Chinese).

Zhang, Y. X., Luo, Y., and Yang, X., 1988, The Panxi Rift: Beijing, China, Geological Press (in Chinese).

Zhou, M. F., Malpas, J., Song, X. Y., Robinson, P. T., Sun, M., Kennedy, A. K., Lesher, C. M., and Keays, R. R., 2002, A temporal link between the Emeishan large igneous province (SW China) and the end-Gaudalupian mass extinction: Earth and Planetary Science Letters, v. 196, p. 51–67.